THE JOURNAL OF BIOLOGICAL CHEMISTRY VOL. 282, NO. 43, pp. 31656–31665, October 26, 2007

Regulation of RGS2 and Second Messenger Signaling in Vascular Smooth Muscle Cells by cGMP-dependent Protein Kinase*[S]

Received for publication, August 1, 2007 Published, JBC Papers in Press, August 6, 2007, DOI 10.1074/jbc.M706360200

Patrick Osei-Owusu[‡1], **Xiaoguang Sun**[‡1], **Ryan M. Drenan**[‡], **Thomas H. Steinberg**[‡§], **and Kendall J. Blumer**[‡2]

From the Departments of [‡]*Cell Biology and Physiology and* [§]*Internal Medicine, Washington University School of Medicine, St. Louis, Missouri 63110*

RGS2, a GTPase-activating protein (GAP) for $G_q\alpha$, regulates vascular relaxation and blood pressure. RGS2 can be phosphorylated by type Iα cGMP-dependent protein kinase (cGKIα), increasing its GAP activity. To understand how RGS2 and cGKIα regulate vascular smooth muscle signaling and function, we identified signaling pathways that are controlled by cGMP in an RGS2-dependent manner and discovered new mechanisms whereby cGK activity regulates RGS2. We show that RGS2 regulates vasoconstrictor-stimulated Ca^{2+} store release, capacitative Ca^{2+} entry, and noncapacitative Ca^{2+} entry and that RGS2 is required for cGMP-mediated inhibition of vasoconstrictor-elicited phospholipase Cβ activation, Ca^{2+} store release, and capacitative Ca^{2+} entry. RGS2 is degraded in vascular smooth muscle cells via the proteasome. Inhibition of cGK activity blunts RGS2 degradation. However, inactivation of the cGKIα phosphorylation sites in RGS2 does not stabilize the protein, suggesting that cGK activity regulates RGS2 degradation by other mechanisms. cGK activation promotes association of RGS2 with the plasma membrane by a mechanism requiring its cGKIα phosphorylation sites. By regulating GAP activity, plasma membrane association, and degradation, cGKIα therefore may control a cycle of RGS2 activation and inactivation. By diminishing cGK activity, endothelial dysfunction may impair RGS2 activation, thereby blunting vascular relaxation and contributing to hypertension.

Signaling by mammalian G protein-coupled receptors (GPCRs)[3] is regulated by a family of at least 30 RGS (regulator of G protein signaling) proteins (1). Most RGS proteins regulate the kinetics and amplitude of G protein signaling in part by functioning as GAPs that accelerate the rate that G protein α subunits hydrolyze GTP and cycle between active and inactive states (2–4). Certain RGS proteins also are Gα-stimulated guanine nucleotide exchange factors (GEFs) for RhoA (5), guanine nucleotide dissociation inhibitors for Gα subunits (6, 7), or binding partners for Rap1 or Rap2 (8), allowing RGS proteins to function as regulators, effectors, and integrators in G protein signaling pathways.

RGS proteins are regulated post-translationally by several mechanisms, including phosphorylation (9–16), lipid binding (17–20), arginylation (21–23), or palmitoylation (24–33). Of these mechanisms, RGS protein phosphorylation is particularly common. Phosphorylation of various RGS proteins can regulate GAP activity (9, 11–13, 34), guanine nucleotide dissociation inhibitor activity (16), degradation (14, 15), or translocation into the nucleus (10). However, the physiological functions served by RGS protein phosphorylation have yet to be established.

Phosphorylation of RGS2 is likely to be critical for regulation of G protein-mediated blood pressure control and vascular relaxation. RGS2 is a potent inhibitor of signaling by $G_q\alpha$ (35, 36), which activates phospholipase Cβ and consequently triggers Ca^{2+} fluxes. RGS2 also has the ability to interact with certain GPCRs, scaffold proteins, and effectors (37–43). RGS2 is likely to regulate GPCR signaling pathways directly involved in blood pressure homeostasis, because it is expressed in vascular smooth muscle and other organs involved in blood pressure control (44–46) and because many vasoconstrictors, including vasopressin, thrombin, and angiotensin II, activate G_q-coupled receptors, thereby promoting myosin light chain phosphorylation and contraction (47–49).

Such evidence led us to discover that $RGS2^{-/-}$ mice are hypertensive (50). Hypertension in $RGS2^{-/-}$ mice is due in part to impaired vascular relaxation in response to NO donors or cGMP analogs (34, 51), which activate cGMP-dependent protein kinases (cGKs) in vascular smooth muscle to attenuate vasoconstrictor signaling and thereby promote relaxation. In the absence of RGS2, these vascular relaxation defects are thought to result from the inability of cGMP to inhibit the Ca^{2+}

* This work was supported by American Heart Association Predoctoral Fellowship 04153107Z (to R. M. D.) and National Institutes of Health Grants GM44592 and HL075632 (to K. J. B.). The costs of publication of this article were defrayed in part by the payment of page charges. This article must therefore be hereby marked "*advertisement*" in accordance with 18 U.S.C. Section 1734 solely to indicate this fact.

[S] The on-line version of this article (available at http://www.jbc.org) contains supplemental Movies 1–4.

[1] These two authors contributed equally to this work and are co-first authors.

[2] To whom correspondence should be addressed: Dept. of Cell Biology and Physiology, Washington University School of Medicine, 660 S. Euclid Ave., St. Louis, MO 63110. Tel.: 314-362-1668; Fax: 314-362-7463; E-mail: kblumer@cellbiology.wustl.edu.

[3] The abbreviations used are: GPCR, G protein-coupled receptor; 8-pCPT-cGMP, 8-(4-chlorophenylthio)guanosine-3′,5′-cyclic monophosphate; Rp-8-pCPT-cGMPS, 8-(4-chlorophenylthio)guanosine-3′,5′-cyclic monophosphorothioate, Rp-isomer; CCE, capacitative (store-operated) Ca^{2+} entry; cGK, cGMP-dependent protein kinase; DAG, diacylglycerol; G protein, guanine nucleotide-binding regulatory protein; GAP, GTPase-activating protein; GEF, guanine nucleotide exchange factor; NCCE, noncapacitative Ca^{2+} entry; PLCβ, phospholipase Cβ; VSMC, vascular smooth muscle cell; GFP, green fluorescent protein; AVP, [Arg[8]]vasopressin.

transients elicited by vasoconstrictors (50, 51). Although specific Ca^{2+} flux pathways regulated by cGMP in an RGS2-dependent manner have yet to be identified, these findings suggest that cGMP activates RGS2 function.

How RGS2 is activated by cGMP stimulation is not clear. RGS2 binds to and is phosphorylated by cGKIα, modestly increasing its GAP activity *in vitro* toward $G_q\alpha$ (~2-fold) (34). However, it is unknown whether this mechanism accounts for cGMP-dependent augmentation of RGS2 function indicated by studies of vasoconstrictor signaling in vascular smooth muscle cells (51). cGMP-stimulated phosphorylation therefore may augment RGS2 activity or function by additional mechanisms.

To elucidate the mechanisms whereby cGMP-triggered phosphorylation regulates vascular smooth muscle function, we have determined the specific vasoconstrictor-triggered Ca^{2+} flux and second messenger pathways that are regulated by cGMP in an RGS2-dependent manner and investigated how cGK-mediated phosphorylation regulates RGS2 in vascular smooth muscle cells. Our findings indicate that cGKIα-mediated phosphorylation regulates the degradation and plasma membrane association of RGS2, which would control RGS2 function as an inhibitor of vasoconstrictor- and G_q-triggered PLCβ activation, Ca^{2+} release, and capacitative Ca^{2+} entry in vascular smooth muscle, thereby promoting vascular relaxation.

EXPERIMENTAL PROCEDURES

Vascular Smooth Muscle Cell (VSMC) Isolation and Culture—All procedures involving animals were performed in strict accordance with protocols approved by the Washington University School of Medicine Animal Studies Committee. Vascular smooth muscle cells (VSMCs) were isolated from thoracic aortas of age-matched (4 months) wild type and $RGS2^{-/-}$ mice, as described previously (50, 51). In brief, freshly isolated aortas were excised and incubated in Dulbecco's modified Eagle's medium/F-12 (Invitrogen). After fatty tissue and blood clots were removed, aortas were diced and enzymatically digested in Dulbecco's modified Eagle's medium/F-12 containing elastase (0.03%, w/v) and collagenase (0.07%, w/v), sieved through 50-mm nylon mesh, washed twice in culture medium, and seeded in a 12-well plate containing poly-L-lysine-coated coverslips. Cells were cultured for 3–5 days in Dulbecco's modified Eagle's medium/F-12 containing 20% fetal bovine serum, 20 ng/ml platelet-derived growth factor, 2 mM glutamine, and 0.1% penicillin and streptomycin. For membrane translocation studies of RGS2, cultured aortic VSMCs from wild type mice were infected with a lentivirus expressing wild type RGS2-myc or mutant RGS2-myc bearing serine to alanine substitutions at the two known cGMP-dependent protein kinase Iα phosphorylation sites (S46A and S64A) and then allowed to grow 48 h before analysis. Staining with anti-smooth muscle α-actin antibody indicated that aortic cell cultures contained ~90% smooth muscle cells (data not shown).

Lentivirus-mediated Expression of RGS2-myc in Primary Aortic VSMCs and Smooth Muscle Cell Lines—We used a lentivirus system to express wild type RGS2-myc and RGS2(S46A,S64A)-myc in primary mouse aortic and cultured A7r5 VSMCs. The viral envelope plasmid VSVG, packaging vector Δ8.9, and transfer vector FCIV were a kind gift from Dr. J. Milbrandt (Washington University School of Medicine). The FCIV vector uses the ubiquitin promoter to drive expression of the gene of interest, followed by an IRES to express enhanced GFP (VENUS) (52). Wild type RGS2-myc and RGS2(S46A,S64A)-myc were cloned into FCIV using the PCR In-fusion™ cloning kit (Clontech) according the manufacturer's protocol. The lentiviral expression system was prepared as previously described (52). Cultured primary aortic and A7r5 VSMCs growing on poly-L-lysine-coated cover glass were infected with lentivirus in the presence of 10 μg/ml Polybrene. After 24 h, the culture medium was replaced, and cells were allowed to grow for 48 h. More than 90% of cells were infected (GFP-positive) as indicated by fluorescence microscopy. Lentivirus-mediated expression of RGS2-myc and RGS2(S46A,S64A)-myc was confirmed by Western blotting using mouse anti-Myc (Covance, Berkeley) and rabbit anti-GFP (AbCam) antibodies.

Ca^{2+} Imaging—Ca^{2+} signaling experiments using primary aortic VSMCs were performed as described previously (50, 51). Briefly, cells grown on coverslips were washed and incubated in 4 μM FURA-2 acetoxymethyl ester (Molecular Probes, Inc., Eugene, OR) in Ca1 solution (11 mM glucose, 130 mM NaCl, 4.8 mM KCl, 1.2 mM $MgCl_2$, 17 mM HEPES, and 1 mM $CaCl_2$, pH 7.3) for 30 min at 37 °C. Cells were washed once and incubated in Ca1 without FURA-2 for 10 min at 37 °C to allow hydrolysis of the acetoxymethyl ester. Cells on coverslips were placed in an open bath recording chamber (Warner Instrument, Hamden, CT) mounted on a Nikon Eclipse E600 FN microscope equipped with a Nikon Fluor ×40/0.80 water immersion lens (Nikon, Melville, NY). Excitation light (340/380 nm) was provided by a TILL Polychrome IV monochrometer (TILL Photonics GmbH, Martinsried, Germany), a 495-nm dichroic mirror, and a 525 ± 20-nm emission filter (Chroma Technology Corp., Brattleboro, VT). For experiments involving cGK activation, VSMCs were mounted in the recording chamber as described above and treated for 10 min with 8-pCPT-cGMP (100 μM), which activates cGKs but does not inhibit phosphodiesterases (53). During subsequent stimulation with vasopressin, 8-pCPT-cGMP (100 μM) was also present. To determine which vasopressin-stimulated Ca^{2+} entry pathways are regulated by RGS2, we incubated cells in Ca1 solution containing $GdCl_3$ (1 μM), which specifically blocks capacitative (store-operated) Ca^{2+} entry (CCE), or SKF 96365 (100 nM), which specifically inhibits noncapacitative Ca^{2+} entry (NCCE) (54–60), and then treated cells with [Arg^8]vasopressin (AVP). To monitor only Ca^{2+} release from intracellular stores, we incubated cells in Ca0 solution (Ca1 lacking Ca^{2+}) and then stimulated cells with AVP. Fluorescence ratio imaging was performed with TILLvisION 4.0 imaging software (TILL Photonics GmbH), and images were acquired with a SensiCam cooled charge-coupled device camera (PCO Computer Optics GmbH, Kelheim, Germany). Regions of interest contained 10–20 VSMCs. Image pairs of the regions of interest were taken every 2 s, and background-corrected ratio images (340 nm/380 nm) were obtained. Data for each region of interest were collected as relative ratio values over time. Ratio data were converted into

$[Ca^{2+}]_i$ by using a standard look-up table created with a Ca^{2+} calibration kit (Molecular Probes).

Monitoring DAG Production by Video Confocal Fluorescence Microscopy—An adenovirus expressing a DAG biosensor consisting of EGFP linked to the DAG-binding C1 domain of PKCγ was constructed and used as follows according to published procedures (61, 62). The plasmid pEGFP-N1-PKCγC1A was a gift of T. Meyer (Sanford University School of Medicine). pShuttle-CMV and pAdEasy-1 vectors in BJ5183 cells were gifts of Dr. H. Piwnica-Worms (Washington University School of Medicine). EGFP-N1-PKCγC1A was subcloned into pShuttle-CMV cleaved with BglII and NotI. The resultant plasmid was linearized by digestion with PmeI and transformed to BJ5183 cells containing pAdEasy-1. The resultant plasmid was cut with PacI and transfected to HEK293 cells, and recombinant adenoviruses expressing EGFP-PKCγC1A were isolated from the culture supernatant. Primary wild type and $RGS2^{-/-}$ vascular smooth muscle cells growing on glass bottom dishes (Bioscience Tools, San Diego, CA) precoated with 0.5 μg/ml vitronectin were infected by adenovirus expressing EGFP-N1-PKCγC1A. After 3 days, the culture medium was replaced with Ca1 solution, and cells were imaged as follows with a laser-scanning confocal microscope (LSM-510; Carl Zeiss MicroImaging, Inc.). Enhanced green fluorescent protein was excited using the 488-nm laser line, and the emitted fluorescence was captured at wavelengths of >505 nm with images collected at 5-s intervals. Wild type and $RGS2^{-/-}$ cells were treated or not with 8-pCPT-cGMP (100 μM for 10 min) and then stimulated with AVP (100 nM). Movies were acquired at 12 frames/min.

Immunofluorescence Microscopy—Primary mouse aortic or A7r5 VSMCs cultured on coverslips were infected with lentiviruses expressing wild type RGS2-myc or RGS2(S46A,S64A)-myc. 48–72 h later, cells were treated with vehicle or 8-pCPT-cGMP (100 μM) or the selective cGKI inhibitor Rp-8-pCPT-cGMPS (20 μM) for 30 min. Cells were fixed with 3% paraformaldehyde in phosphate-buffered saline for 30 min, washed, and blocked with 5% normal goat serum in buffer A (phosphate-buffered saline with 0.1% Triton X-100) for 20 min at 4 °C. Cells were incubated with primary antibodies (1:100 mouse anti-Myc, 9E10; Covance, Berkeley, CA) in buffer A with 1% goat serum for 20 min and washed 10 times. Secondary antibodies (1:1000 Alexa Fluor488 goat anti-mouse IgG; Molecular Probes) in solution A with 1% goat serum were incubated with cells for 20 min, followed by 10 washes in buffer A, and examined by confocal fluorescence microscopy. Fluorescence images were quantified using NIH Image J 1.37v. The proportion of wild type or mutant RGS2-myc associated with the plasma membrane was quantified on a cell by cell basis by subtracting the fluorescence signal in the cytoplasm/intracellular organelles/nucleus from the total fluorescence of the cell and dividing this value by total fluorescence.

RGS2-myc Degradation—A7r5 smooth muscle cells grown to ~70% confluence in Dulbecco's modified Eagle's medium/F-12 supplemented with 10% fetal bovine serum and 2 mM glutamine were transfected using FUGENE 6 reagent and FCIV transfer plasmid expressing RGS2-myc or RGS2(S46A,S64A)-myc. 48 h after transfection, cells were treated with vehicle, 8-pCPT-cGMP (100 μM), or Rp-8-pCPT-cGMPS (20 μM) in the presence of cycloheximide (30 μg/ml). The proteasome dependence of RGS2-myc degradation was investigated by treating cells with MG132 (10 μM). Cells were harvested by the addition of ice-cold phosphate-buffered saline and lysed in MLCB (50 mM Tris, pH 8.0, 2 mM dithiothreitol, 5 mM EDTA, 0.5% Nonidet P-40, 100 mM NaCl, 1 μM microcystin, 1 mM sodium orthovanadate, 1 mM phenylmethylsulfonyl fluoride) supplemented with protease inhibitor tablets (Roche Applied Science). Cell debris and unbroken cells were pelleted by centrifugation (13,000 × *g*) for 15 min at 4 °C. Supernatant fractions were used for Western blotting (30 μg of total protein/lane separated on 12% SDS-polyacrylamide gels and transferred to polyvinylidene difluoride membranes (Millipore)). Membranes were blocked for 1 h in 5% fat-free milk/TBST followed by co-incubation with primary antibodies (1:1000 mouse anti-Myc, 9E10 (Covance); 1:2000 rabbit anti-GFP (AbCam)) overnight at 4 °C. Membranes were washed and co-incubated with secondary antibodies conjugated with infrared fluorescent dyes (1:10,000 goat anti-mouse IRDye680® and 1:10,000 goat anti-rabbit IRDye® 800CW; LI-COR Biosciences, Lincoln, NE) for 1 h. Myc and GFP bands were detected and quantified using an Odyssey infrared imaging system (LI-COR Biosciences). RGS2-myc protein expression was normalized to that of co-expressed GFP.

Statistics—Student's *t* test (two-tailed, two-sample, equal variance) with Bonferroni correction was used to analyze Ca^{2+} signaling data, the effect of proteasome inhibitor on RGS2-myc degradation, and membrane translocation data. A two-way analysis of variance was used to assess the effect of 8-pCPT-cGMP and Rp-pCPT-cGMPS on the degradation rate of RGS2-myc and RGS2(S46A,S64A)-myc proteins at various time points. A Newman-Keuls *post hoc* test was used to determine between-group differences at the various time points. A *p* value of less than 0.05 was considered statistically significant.

RESULTS

RGS2 Regulates Vasopressin-stimulated Ca^{2+} Store Release and Entry in Primary Aortic Vascular Smooth Muscle Cells—To determine whether RGS2 regulates specific Ca^{2+} release and/or Ca^{2+} entry mechanisms in VSMCs stimulated by AVP, we used specific pharmacologic tools established by previous investigations (54–60). Our objective was to determine whether RGS2 regulates AVP-triggered Ca^{2+} release from intracellular stores, CCE, or NCCE. An answer to this question was required to determine whether RGS2 negatively regulates Ca^{2+} flux pathways implicated in vascular contraction and to determine which Ca^{2+} flux pathways are inhibited by the NO-cGMP pathway in an RGS2-dependent manner in order to promote relaxation. We used congenic wild type and $RGS2^{-/-}$ mice to prepare primary aortic smooth muscle cells, as described previously (50, 51). We did not routinely use primary smooth muscle cells from mesenteric resistance arteries, because they were difficult to isolate in sufficient quantity and because aortic and mesenteric artery smooth muscle cells gave equivalent results in preliminary experiments (51) (data not shown).

Contributions of Ca^{2+} release from internal stores, CCE, and NCCE to total Ca^{2+} fluxes elicited by AVP were investigated by performing FURA-2 imaging experiments using VSMCs

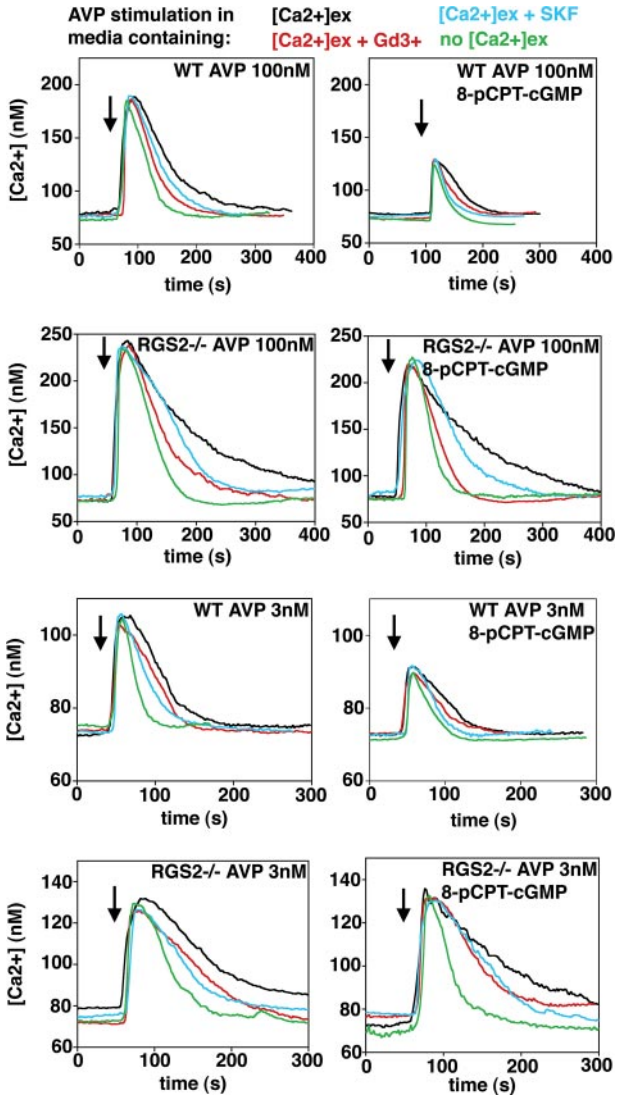

FIGURE 1. **AVP-stimulated Ca^{2+} fluxes in wild type (*WT*) and $RGS2^{-/-}$ aortic VSMCs.** FURA-2 imaging of AVP-stimulated intracellular Ca^{2+} fluxes was performed as indicated under the following conditions: Ca^{2+}-containing media ([Ca^{2+}]*ex*) with no inhibitors; inhibition of CCE by Gd^{3+} (1 μM); inhibition of NCCE by SKF 96365 (100 nM); absence of Ca^{2+} entry due to lack of Ca^{2+} in the medium (*no* [Ca^{2+}]*ex*). Ca^{2+} fluxes stimulated were under these conditions by the indicated concentrations of AVP in wild type and $RGS2^{-/-}$ primary aortic VSMCs in the absence and presence of 8-pCPT-cGMP (100 μM for this and all subsequent experiments), as indicated. The *arrow* in each *panel* indicates the time at which AVP was applied. The results shown are the average of 3–5 experiments (10–20 cells/field each) performed under each condition.

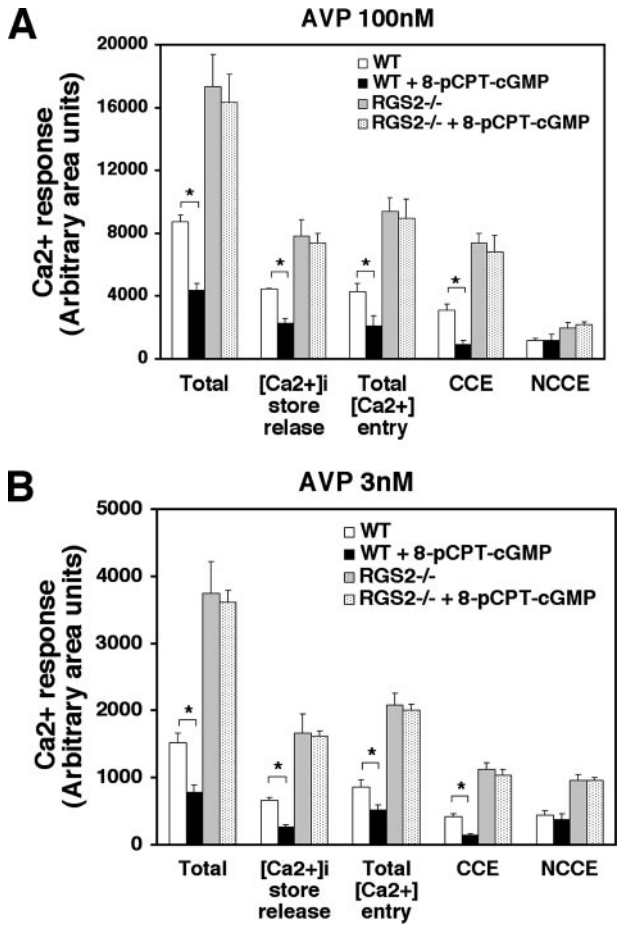

FIGURE 2. **The absence of RGS2 augments AVP-stimulated Ca^{2+} release, CCE, and NCCE and blocks the ability of a cGK activator to inhibit AVP-stimulated Ca^{2+} release and CCE.** Data shown in Fig. 1 were analyzed and quantified as described under "Experimental Procedures" to determine the portion of the total AVP-stimulated Ca^{2+} response that was due to intracellular store release, total Ca^{2+} entry, CCE, or NCCE in wild type (*white* and *black bars*) or $RGS2^{-/-}$ (*gray* and *stippled bars*) aortic VSMCs in the absence (*white* and *gray bars*) or presence (*black* and *stippled bars*) of the cGK activator 8-pCPT-cGMP. *A*, Ca^{2+} responses triggered by a saturating concentration of AVP (100 nM), which triggers CCE more strongly than NCCE. *B*, Ca^{2+} responses triggered by a low concentration of AVP (3 nM), which favors NCCE relative to CCE. The *error bars* indicate S.E. *, $p < 0.05$. *WT*, wild type.

treated in the following ways, as established previously (54–60). Primary aortic VSMCs from wild type and $RGS2^{-/-}$ mice were incubated in the following media: 1) containing Ca^{2+} (*black curves* in Fig. 1) to monitor total Ca^{2+} flux; 2) lacking Ca^{2+} (*green curves*) to detect only Ca^{2+} release from intracellular stores; 3) containing Ca^{2+} and Gd^{3+} (1 μM; *red curves*) to inhibit CCE but not NCCE or Ca^{2+} release from intracellular stores; and 4) containing Ca^{2+} and SKF 96365 (100 nM; *cyan curves*) to block NCCE but not CCE or Ca^{2+} release. Although Gd^{3+} and SKF 96365 currently provide the best pharmacological tools to probe CCE and NCCE, they can inhibit a variety of Ca^{2+} or cation channels. Thus, it was important to confirm that these compounds discriminated between CCE and NCCE. Accordingly, we stimulated cells treated as described above under conditions known to augment (3 nM AVP) or diminish (100 nM AVP) NCCE relative to CCE (54–60). All experiments were conducted using cells treated or not with the cell-permeant cGMP analog 8-pCPT-cGMP (10 min prior to the AVP addition) to determine which Ca^{2+} flux pathways are inhibited acutely by cGMP stimulation in an RGS2-dependent manner. This cGMP analog activates cGKs but does not inhibit phosphodiesterases that would affect cGMP and cAMP levels (53).

Results of experiments measuring Ca^{2+} fluxes triggered by AVP are shown in Figs. 1 and 2. Fig. 1 shows the average time courses of AVP-stimulated Ca^{2+} fluxes observed in wild type and $RGS2^{-/-}$ cells under each condition described above. Total Ca^{2+} response was defined as the response obtained in media containing Ca^{2+} and no inhibitors. Ca^{2+} release from intracellular stores was defined as the response obtained in the absence of extracellular Ca^{2+}. Total Ca^{2+} influx from the medium (*i.e.* CCE + NCCE) was defined as the total Ca^{2+}

response minus the Ca^{2+} response due to store release. CCE was defined as the Ca^{2+} response in media containing Ca^{2+} and NCCE blocker (SKF 96365) minus the Ca^{2+} response due to store release. NCCE was defined as the Ca^{2+} response in media containing Ca^{2+} and CCE blocker (Gd^{3+}) minus the Ca^{2+} response due to store release. These data were quantified by integrating the area under each curve in Fig. 1 to determine the magnitude of the Ca^{2+} response contributed collectively by all mechanisms or separately by release from intracellular stores, CCE, or NCCE, as shown in Fig. 2.

Results quantified in Fig. 2 indicated several observations. First, as expected from previous studies of VSMC lines (55–58), the contribution of NCCE relative to CCE was greater at low concentrations of AVP, confirming the validity of methods used to selectively inhibit CCE *versus* NCCE. Second, the absence of RGS2 significantly augmented AVP-stimulated Ca^{2+} release, CCE, and NCCE. This result suggested that RGS2 limits the magnitude and/or duration of AVP-stimulated G_q activity and consequent production of inositol 1,4,5-trisphosphate and diacylglycerol by the action of PLCβ. Third, in wild type cells, 8-pCPT-cGMP strongly inhibited AVP-triggered Ca^{2+} release and CCE but had an insignificant effect on AVP-stimulated NCCE. Fourth, in RGS2$^{-/-}$ cells, 8-pCPT-cGMP failed to inhibit AVP-triggered Ca^{2+} release, CCE, or NCCE. These latter two results indicated that RGS2 is essential for cGMP-mediated inhibition of AVP-triggered Ca^{2+} release and CCE, thereby establishing a mechanism for the vascular relaxation impairment observed in RGS2$^{-/-}$ mice.

RGS2 Mediates cGMP-triggered Inhibition of Vasopressin-stimulated PLCβ Activation—The preceding results are consistent with the hypothesis that RGS2 regulates AVP-stimulated Ca^{2+} fluxes by controlling G_q-mediated PLCβ activation. However, because RGS2 has targets other than G_q (reviewed in Refs. 45 and 46) and because Ca^{2+} flux pathways are complex and subject to incompletely understood regulatory mechanisms (reviewed in Ref. 63), it was essential to determine directly whether RGS2 regulates AVP- and G_q-stimulated PLCβ activity in VSMCs.

Accordingly, we employed a biosensor of PLCβ-stimulated diacylglycerol (DAG) production consisting of GFP fused to the DAG-binding C1 domain of PKCγ (EGFP-N1-PKCγC1A or GFP-C1), which translocates from the cytoplasm to the plasma membrane in response to DAG production via PLCβ action (64). We expressed GFP-C1 by adenoviral infection of primary aortic smooth muscle cells from wild type and RGS2$^{-/-}$ mice. Cells were analyzed 3 days after infection by confocal fluorescence video microscopy to follow the time course of AVP-stimulated DAG production in the absence or presence of 8-cPT-cGMP.

Fig. 3 shows representative frames of movies (movies are available in the Supplemental materials) of AVP-stimulated GFP-C1 translocation in AVP-stimulated wild type and RGS2$^{-/-}$ aortic VSMCs. In the absence of 8-pCPT-cGMP, GFP-C1 translocated efficiently to the plasma membrane when wild type or RGS2$^{-/-}$ cells were stimulated with AVP. These cells also exhibited AVP-stimulated membrane ruffling and microspike formation (see movies in the supplemental materials). In contrast, in wild type cells pretreated with 8-pCPT-cGMP, AVP failed to trigger translocation of GFP-C1 or cell shape changes (see Fig. 3 and supplemental materials). Strikingly, however, in RGS2$^{-/-}$ cells treated with 8-pCPT-cGMP, AVP stimulated robust translocation of C1-GFP and membrane ruffling (Fig. 3 and supplemental materials). Therefore, RGS2 is required for cGMP-mediated inhibition of AVP-stimulated PLCβ activation and consequent cell shape changes.

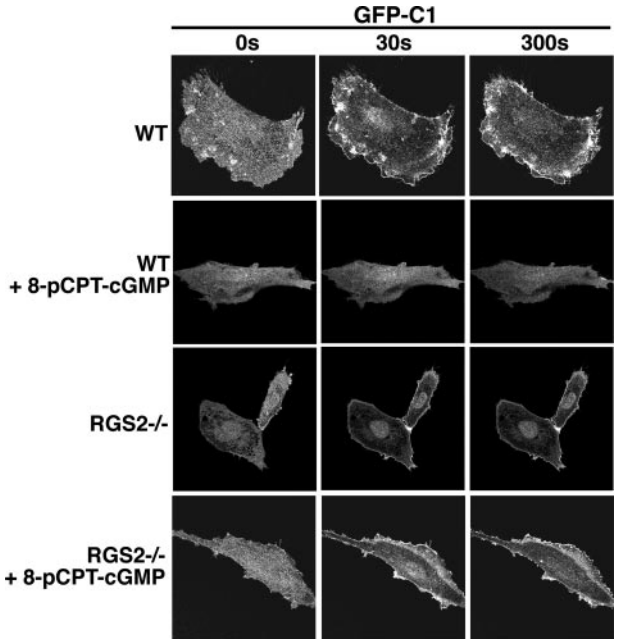

FIGURE 3. **RGS2 is required for a cGK activator to inhibit AVP-stimulated phospholipase Cβ activation.** A biosensor of AVP-stimulated phospholipase Cβ activation consisting of the DAG-binding C1 domain of PKCγ (GFP-C1) was expressed by adenoviral infection of primary aortic VSMCs from wild type (*WT*) and RGS2$^{-/-}$ mice. Cells stimulated with AVP for the indicated times in the absence or presence of the cGK activator 8-pCPT-cGMP were analyzed by confocal video fluorescence microscopy. Representative frames acquired at the indicated times before (0 s) or after AVP stimulation are shown. The results shown are representative of three experiments. Movies are available in the supplemental materials.

cGK Inhibition Attenuates RGS2 Degradation in Vascular Smooth Muscle Cells—To determine whether cGKIα-mediated phosphorylation regulates RGS2 function in cells by mechanisms other than by increasing its GAP activity, we transfected A7r5 vascular smooth muscle cells with a plasmid that co-expresses a functional Myc-tagged form of RGS2 and a variant of green fluorescent protein (VENUS). This approach allowed us to determine efficiency of transfection and normalize expression of RGS2-myc relative to VENUS for studies of protein degradation rates. A7r5 cells were used instead of primary mouse aortic smooth muscle cells, because protein degradation studies required large numbers of cells.

Results shown in Fig. 4 indicate that a cGK inhibitor decreases the rate of RGS2-myc degradation in A7r5 smooth muscle cells. In cells treated with the selective and potent cGK inhibitor (Rp-8-pCPT-cGMPS) (65) and cycloheximide to block new protein synthesis, RGS2-myc degradation over time was slower relative to cells treated with vehicle and cycloheximide (Fig. 4*A*). Stimulation of cells with a selective cGK activator (8-pCPT-cGMP) did not augment the rate of RGS2-myc degradation relative to vehicle controls (Fig. 4*A*). In the absence of a cGK inhibitor, degradation of wild type RGS2-myc in A7r5

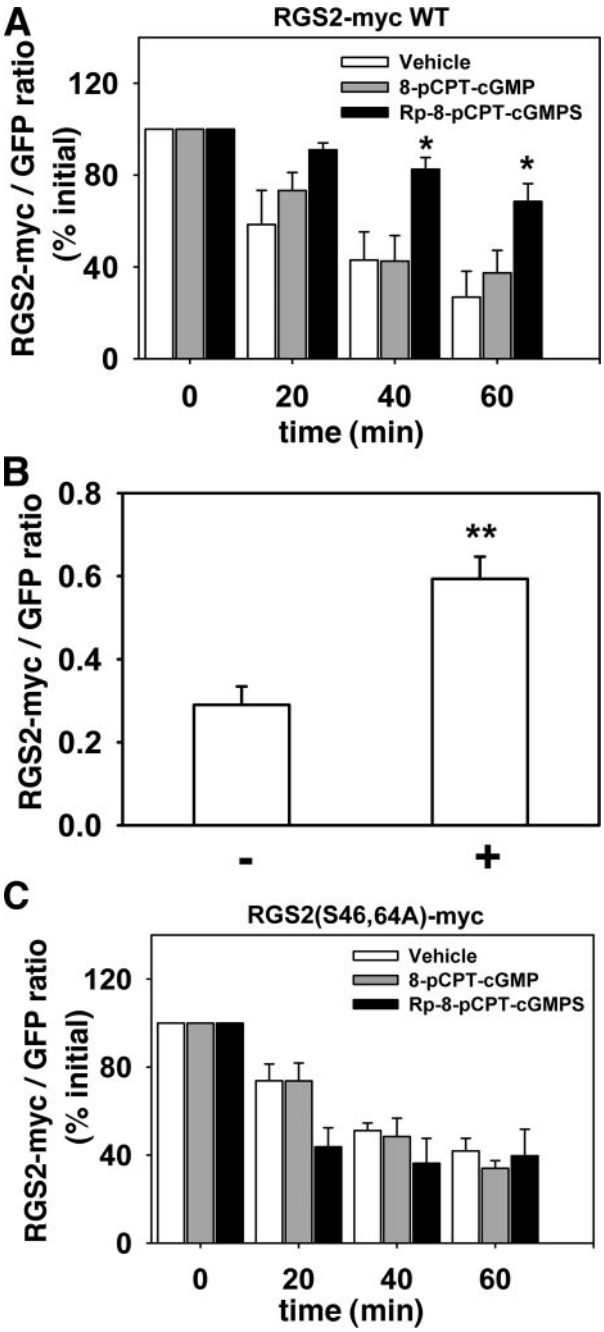

FIGURE 4. **cGK-regulated degradation of RGS2 in vascular smooth muscle cells.** Wild type (*WT*) RGS2-myc and RGS2(S46A,S64A)-myc lacking the two known cGKIα phosphorylation sites were co-expressed with a GFP variant (VENUS) by transfection of A7r5 vascular smooth muscle cells. *A*, a cGK inhibitor blunts degradation of wild type RGS2-myc. A7r5 cells co-expressing wild type RGS2-myc and GFP were treated with cycloheximide (30 μg/ml) plus vehicle (*open bars*), the cGK activator 8-pCPT-cGMP (100 μM; *gray bars*), or the cGK inhibitor Rp-8-pCPT-cGMPS (20 μM; *black bars*) and analyzed by Western blotting to quantify the RGS2-myc/GFP ratio over time. *B*, degradation of wild type RGS2-myc is sensitive to a proteasome inhibitor. The ratio of wild-type RGS2-myc/GFP was quantified in cells treated for 1 h with cycloheximide in the presence or absence of the proteasome inhibitor MG-132 (10 μM). *C*, RGS2 degradation is not blocked by inactivating its two known cGKIα phosphorylation sites. Cells co-expressing RGS2(S46A,S64A)-myc and GFP were treated with cycloheximide (30 μg/ml) plus vehicle (*open bars*), the cGK activator 8-pCPT-cGMP (100 μM; *gray bars*), or the cGK inhibitor Rp-8-pCPT-cGMPS (20 μM; *black bars*) and analyzed by Western blotting to quantify the RGS2-myc/GFP ratio over time. Results shown in each *panel* are the average of at least three experiments performed in duplicate. The *error bars* indicate S.E. *, $p < 0.05$ relative to values of obtained with vehicle- and 8-pCPT-cGMP-treated cells. **, $p < 0.01$ relative to values obtained with vehicle-treated cells.

cells appears to be mediated by the proteasome, because the levels of RGS2-myc were significantly higher in cells incubated for 1 h with cycloheximide and the proteasome inhibitor MG132 relative to cells treated only with cycloheximide (Fig. 4*B*). Because the N-terminal domain of RGS2 fused to GST can be phosphorylated *in vitro* on serine 46 and serine 64 by cGKIα (34), we determined whether these phosphorylation sites regulate the degradation of full-length RGS2-myc in A7r5 cells. If phosphorylation of these sites promotes degradation of RGS2-myc, then this mutant form of RGS2-myc should be degraded slowly, like wild type RGS2-myc in the presence of the cGK inhibitor. Contrary to this expectation, under all conditions tested (vehicle, cGK inhibitor, or cGK activator), we found that mutant RGS2-myc was degraded rapidly (Fig. 4*C*), like wild type RGS2-myc in the absence of the cGK inhibitor. This result indicated that the mechanisms whereby cGK activity controls RGS2 degradation are complex (see "Discussion").

cGK Regulation RGS2 Association with the Plasma Membrane in Vascular Smooth Muscle Cells—Two lines of evidence prompted us to investigate whether cGK-mediated phosphorylation regulates the intracellular localization of RGS2 in VSMCs. First, cGKIα phosphorylation sites (serine 46 and serine 64) (34, 66) are located within or near an N-terminal amphipathic α-helical membrane-targeting domain of RGS2 (residues 32–66) (67). Second, because the N-terminal domain of RGS2 fused to GFP associates efficiently with the plasma membrane, whereas full-length RGS2 does not (67), the membrane association function of the amphipathic helix in full-length RGS2 may be regulated.

To test this hypothesis, we used lentiviruses to express wild type or mutant RGS2-myc lacking its two known cGKIα phosphorylation sites (S46A,S64A mutant) in primary mouse aortic and A7r5 VSMCs. Infected cells were treated for 30 min with or without a cGK activator (8-pCPT-cGMP) or cGK inhibitor (Rp-8-pCPT-cGMPS) and analyzed by confocal immunofluorescence microscopy to determine the localization of RGS2-myc (Fig. 5). Data obtained with primary aortic VSMCs were quantified (Fig. 6; see "Experimental Procedures") to determine the proportion of the total RGS2-myc pool that was plasma membrane-associated. The results indicated that under control conditions, wild type RGS2-myc associated detectably with the plasma membrane. In cells treated with the cGK activator (8-pCPT-cGMP), the fraction of the total wild type RGS2-myc pool that was plasma membrane-localized increased significantly (Fig. 6). Conversely, treating cells with the cGK inhibitor (Rp-8-pCPT-cGMPS) decreased the association of wild type RGS2-myc with the plasma membrane (Fig. 6). The effects of the cGK activator and inhibitor on RGS2-myc localization were specific, because activation of PKC, which can phosphorylate RGS2 (12), did not affect RGS2-myc localization (data not shown). In contrast to what we observed with cells expressing wild type RGS2-myc, both the cGK activator (8-pCPT-cGMP) and inhibitor (Rp-8-pCPT-cGMPS) reduced the proportion of RGS2(S46A,S64A)-myc associated with the plasma membrane (Fig. 6). These two known cGKIα phosphorylation sites therefore appeared to be required for augmented plasma membrane localization of RGS2-myc in

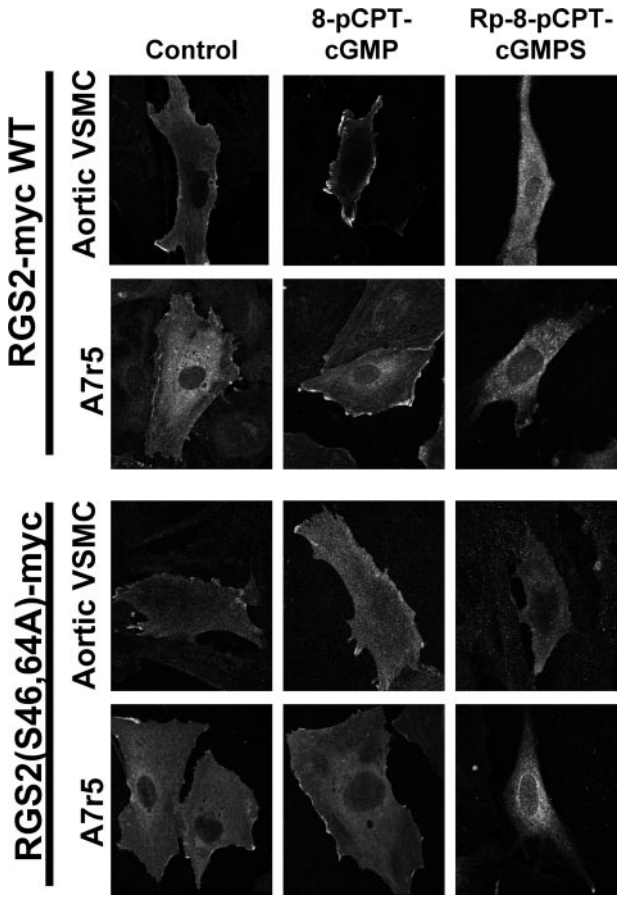

FIGURE 5. **Localization of RGS2 in vascular smooth muscle cells is regulated by cGK activity.** Shown are confocal fluorescence microscopy images of primary mouse aortic and A7r5 VSMCs infected with lentivirus expressing wild type RGS2-myc or mutant RGS2(S46A,S64A)-myc treated for 30 min with or without the cGK activator 8-pCPT-cGMP or the cGKI inhibitor Rp-8-pCPT-cGMPS. >80% of cells ($n > 20$ for each condition) displayed the localization patterns shown.

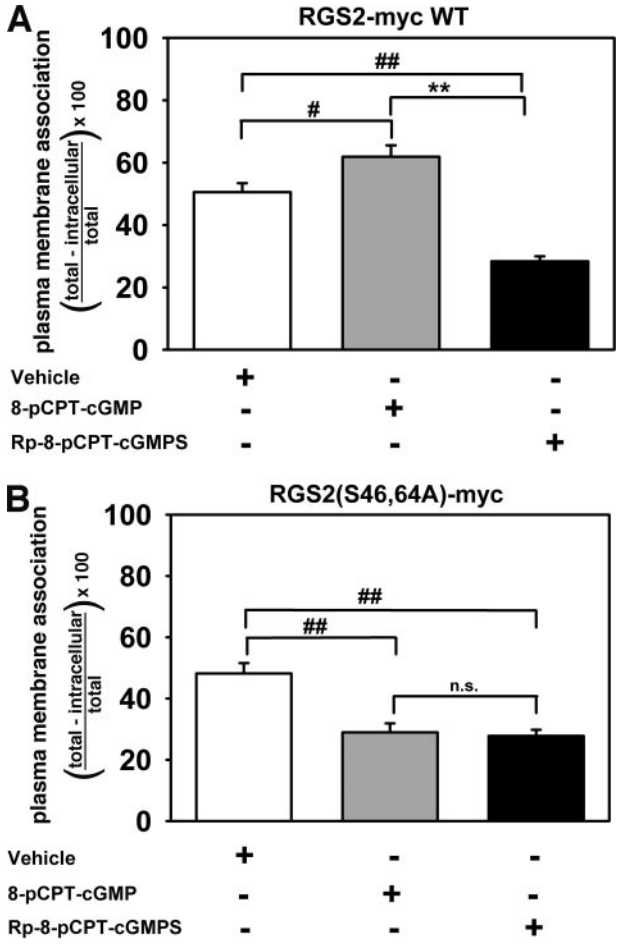

FIGURE 6. **cGK activity regulates plasma membrane association of RGS2 in vascular smooth muscle cells.** Association of wild type (*WT*) RGS2-myc or RGS2(S46A,S64A)-myc with the plasma membrane of primary mouse aortic smooth muscle cells was quantified from confocal fluorescence micrographs as described under "Experimental Procedures." *A*, effects of vehicle, the cGK activator 8-pCPT-cGMP, and cGK inhibitor Rp-8-pCPT-cGMPS on the association of wild type RGS2-myc on the plasma membrane. *B*, effects of vehicle, the cGK activator 8-pCPT-cGMP, and cGK inhibitor Rp-8-pCPT-cGMPS on the association of RGS2(S46A,S64A)-myc on the plasma membrane. Results shown are the average of duplicate experiments that examined at least 15 cells under each experimental condition. *Error bars*, S.E. **, $p < 0.01$ (8-pCPT-cGMP *versus* Rp-8-pCPT-cGMPS); #, $p < 0.05$ (vehicle *versus* 8-pCPT-cGMP); ##, $p < 0.01$ (vehicle *versus* Rp-8-pCPT-cGMPS). *n.s.*, not significant.

response to cGK activation. However, because the cGK activator and inhibitor both reduced the plasma membrane association of RGS2(S46A,S64A)-myc, cGK activity apparently regulates the plasma membrane association of RGS2-myc by additional mechanisms (see "Discussion"). Taken together, these results and those of previous studies indicate that RGS2 GAP activity, degradation, and localization are regulated by cGK activity.

DISCUSSION

Regulation of Vasoconstrictor-triggered Ca^{2+} Flux Pathways by RGS2 and cGMP—Results presented herein demonstrate that RGS2 is a crucial effector of the NO-cGMP pathway that promotes vascular relaxation by inhibiting vasoconstrictor-mediated PLCβ activation and Ca^{2+} signaling. We have found in aortic smooth muscle cells that the inhibitory effects of a cGMP analog on vasoconstrictor (vasopressin)-induced PLCβ activation, Ca^{2+} release from intracellular stores, and CCE are essentially completely dependent on the presence of RGS2. This finding therefore establishes a mechanism for impaired NO- or cGMP-triggered vascular relaxation in $RGS2^{-/-}$ mice (34, 51). However, in the absence of RGS2, why is cGMP-mediated inhibition of AVP-stimulated Ca^{2+} release and CCE essentially completely defective, whereas NO- or cGMP-triggered vascular relaxation is impaired but not completely defective? A straightforward possibility is that RGS2 is dispensable for cGMP-mediated inhibition of vasoconstrictor-triggered RhoA activation and signaling. We suggest this hypothesis, because cGMP analogs inhibit the ability of vasoconstrictor receptors to activate RhoA via $G_{12/13}$ (68), which are insensitive to inhibition by RGS2. Thus, in the absence of RGS2, the NO-cGMP pathway is expected to retain the ability to inhibit the RhoA pathway, thereby allowing relaxation to occur, albeit with reduced efficiency.

Our analysis of cGMP regulation of PLCβ activation and Ca^{2+} signaling in wild type *versus* $RGS2^{-/-}$ VSMCs raises the possibility that a novel pathway exists whereby vasopressin receptors trigger NCCE. We suggest this hypothesis based on the following information. Previous investigations have indicated that vasopressin stimulates NCCE in vascular

smooth muscle cells by a pathway in which DAG produced by PLCβ action is converted to arachidonic acid, which stimulates NO production and triggers NCCE (54–58). Consistent with this mechanism, our results indicate that NCCE is augmented in cells lacking RGS2, as expected if RGS2 negatively regulates G_q-stimulated PLCβ activation and consequent DAG production. However, if this pathway provides the sole means of triggering NCCE, it should be inhibited by cGMP analogs in an RGS2-dependent manner. In contrast, we find that 8-pCPT-cGMP insignificantly inhibits vasopressin-triggered NCCE, whether RGS2 is present or absent. Accordingly, vasopressin receptors may trigger NCCE by another mechanism that is insensitive to inhibition by RGS2, possibly involving $G_{12/13}$ or G protein-independent pathways.

RGS2 Regulation by cGMP-dependent Protein Kinase—We have discovered two new mechanisms whereby cGK activity regulates RGS2 in vascular smooth muscle cells. First, whereas RGS2 is an unstable protein that is degraded via the proteasome, its degradation is blunted when vascular smooth muscle cells are treated with a cGK inhibitor. The mechanism by which cGK activity regulates RGS2 degradation is not clear, because a cGK activator does not stimulate RGS2 degradation, perhaps because basal cGK activity is sufficient to promote RGS2 degradation. Moreover, an RGS2 mutant lacking the two known cGKIα phosphorylation sites (S46A,S64A) is degraded rapidly whether cells are treated with a cGK activator or inhibitor, suggesting that dephosphorylation of these sites is insufficient to stabilize RGS2. Nevertheless, this mutant form of RGS2 could adopt an abnormal conformation, rendering it more susceptible to degradation. Therefore, further work will be required to dissect the precise mechanisms whereby cGK activity regulates RGS2 degradation. However, such mechanisms may be relevant to human hypertension, because a rare *Rgs2* allele (Q2L) identified in a Japanese hypertensive population promotes RGS2 degradation (69).

Second, we have found that cGK activity regulates the intracellular localization of RGS2 in vascular smooth muscle cells. Whereas a cGK activator augments the association of RGS2 with the plasma membrane, a cGK inhibitor has the opposite effect. In contrast, plasma membrane association of RGS2 lacking its cGKIα phosphorylation sites is inhibited in response to either a cGK activator or inhibitor. Therefore, although these cGKIα phosphorylation sites are partially responsible for mediating the effects of cGK activity on RGS2 localization, other mechanisms may also be involved. For example, cGK may phosphorylate RGS2 on other sites or phosphorylate other proteins that bind RGS2 and influence its association with the membrane. Indeed, RGS2 can interact with overexpressed $G_q\alpha$, $G_s\alpha$, spinophilin, adenylyl cyclase, TRPV6, and certain GPCRs (38, 40, 42, 43, 70, 71).

How might cGK-mediated phosphorylation trigger recruitment of RGS2 to the plasma membrane? Based on a structural model of full-length membrane-bound RGS2 developed by molecular dynamics modeling and other methods (72), we hypothesize that cGKIα-mediated phosphorylation of RGS2 regulates the structure or accessibility of the N-terminal domain, which contains the two cGKIα phosphorylation sites (Ser^{46} and Ser^{64}) and an amphipathic α-helical membrane-targeting domain (residues 32–66). In this structural model (Fig. 7), Ser^{46} and Lys^{41} are located on the hydrophilic face of the amphipathic helix such that Ser^{46} phosphorylation could allow these two residues to form a salt bridge that stabilizes the amphipathic helix and promotes membrane binding. Alternatively, Ser^{46} phosphorylation potentially promotes salt bridge formation with Lys^{71} in a loop connecting the amphipathic helix and the RGS domain (Fig. 7), which also could stabilize the amphipathic helix. Ser^{64} is located in the connecting loop between the amphipathic helix and the RGS domain, where it potentially interacts, when phosphorylated, with Lys^{57}, Lys^{63}, or Lys^{65} in the loop (Fig. 7), possibly altering the conformation of the N-terminal domain and exposing the amphipathic helix for membrane binding.

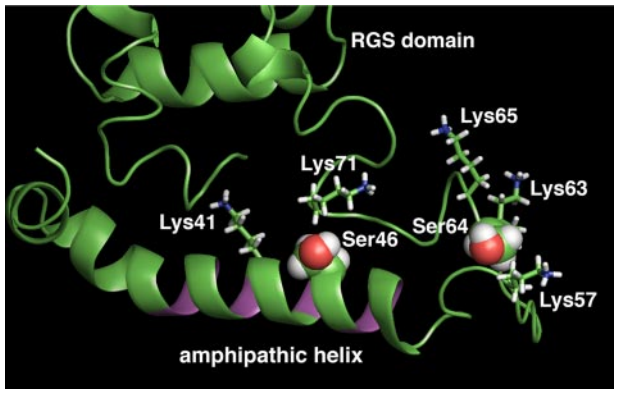

FIGURE 7. **Proposed mechanism of RGS2 membrane targeting triggered by cGKIα phosphorylation.** A structural model of full-length RGS2 optimized for membrane binding is shown (72). Residues of RGS2 (Ser^{46} and Ser^{64}) that are phosphorylated by cGKIα and are required for cGMP-triggered translocation to the plasma membrane are indicated in a *space fill representation*. Basic residues hypothesized to form charged pair interactions with phosphorylated Ser^{46} and Ser^{64} are indicated as *sticks*. The hydrophobic face of the amphipathic membrane-targeting helix is indicated in *purple*. Charged pair interactions involving the indicated basic residues and phosphorylated Ser^{46} and Ser^{64} are hypothesized to stabilize the amphipathic helix in a conformation that promotes membrane binding. For clarity, only a portion of the RGS domain is shown. See "Discussion" for details.

In conclusion, our studies and previous investigations suggest a model whereby a cycle of RGS2 activation and deactivation in vascular smooth muscle cells is controlled by cGK activity. In this model, RGS2 is an unstable protein that under basal conditions has low GAP activity and associates relatively inefficiently with the plasma membrane. Following cGK activation, RGS2 GAP activity and plasma membrane association increase, augmenting the ability of RGS2 to deactivate $G_q\alpha$. RGS2-mediated deactivation of $G_q\alpha$ would impair the ability of vasoconstrictor receptors to activate PLC-β, thereby attenuating production of DAG and IP3, release of Ca^{2+} from intracellular stores, and Ca^{2+} entry via CCE. As cGMP levels fall, cGK activity would decline, and RGS2 would return to a state with lower GAP activity and reduced affinity for the plasma membrane, thereby disinhibiting vasoconstrictor-mediated G_q signaling and promoting vascular contraction. Because in human hypertension, the activity of the NO-cGMP pathway and cGKIα often are reduced due to endothelial dysfunction (reviewed in Ref. 73),

impaired activation of RGS2 may occur and contribute to vascular relaxation defects and elevated blood pressure.

Acknowledgments—We thank K. Kaltenbronn for providing superb technical support; I. Tikhonova and D. Fourmy (INSERM, Toulouse, France) for kindly providing the coordinates of the RGS2 structural model; Craig Press for providing advice with lentivirus protocols; and H. Teng, A. Muslin, M. Linder, and members of the Blumer laboratory for contributing advice and discussion.

REFERENCES

1. Hollinger, S., and Hepler, J. R. (2002) *Pharmacol. Rev.* **54,** 527–559
2. Berman, D. M., Wilkie, T. M., and Gilman, A. G. (1996) *Cell* **86,** 445–452
3. Hunt, T. W., Fields, T. A., Casey, P. J., and Peralta, E. G. (1996) *Nature* **383,** 175–177
4. Watson, N., Linder, M. E., Druey, K. M., Kehrl, J. H., and Blumer, K. J. (1996) *Nature* **383,** 172–175
5. Hart, M. J., Jiang, X., Kozasa, T., Roscoe, W., Singer, W. D., Gilman, A. G., Sternweis, P. C., and Bollag, G. (1998) *Science* **280,** 2112–2114
6. Hollinger, S., Taylor, J. B., Goldman, E. H., and Hepler, J. R. (2001) *J. Neurochem.* **79,** 941–949
7. Kimple, R. J., De Vries, L., Tronchere, H., Behe, C. I., Morris, R. A., Gist Farquhar, M., and Siderovski, D. P. (2001) *J. Biol. Chem.* **276,** 29275–29281
8. Traver, S., Bidot, C., Spassky, N., Baltauss, T., De Tand, M. F., Thomas, J. L., Zalc, B., Janoueix-Lerosey, I., and Gunzburg, J. D. (2000) *Biochem. J.* **350,** 19–29
9. Balasubramanian, N., Levay, K., Keren-Raifman, T., Faurobert, E., and Slepak, V. Z. (2001) *Biochemistry* **40,** 12619–12627
10. Burgon, P. G., Lee, W. L., Nixon, A. B., Peralta, E. G., and Casey, P. J. (2001) *J. Biol. Chem.* **276,** 32828–32834
11. Chen, C., Wang, H., Fong, C. W., and Lin, S. C. (2001) *FEBS Lett.* **504,** 16–22
12. Cunningham, M. L., Waldo, G. L., Hollinger, S., Hepler, J. R., and Harden, T. K. (2001) *J. Biol. Chem.* **276,** 5438–5444
13. Derrien, A., and Druey, K. M. (2001) *J. Biol. Chem.* **276,** 48532–48538
14. Derrien, A., Zheng, B., Osterhout, J. L., Ma, Y. C., Milligan, G., Farquhar, M. G., and Druey, K. M. (2003) *J. Biol. Chem.* **278,** 16107–16116
15. Garrison, T. R., Zhang, Y., Pausch, M., Apanovitch, D., Aebersold, R., and Dohlman, H. G. (1999) *J. Biol. Chem.* **274,** 36387–36391
16. Hollinger, S., Ramineni, S., and Hepler, J. R. (2003) *Biochemistry* **42,** 811–819
17. Ishii, M., Inanobe, A., and Kurachi, Y. (2002) *Proc. Natl. Acad. Sci. U. S. A.* **99,** 4325–4330
18. Ouyang, Y. S., Tu, Y., Barker, S. A., and Yang, F. (2003) *J. Biol. Chem.* **278,** 11115–11122
19. Popov, S. G., Krishna, U. M., Falck, J. R., and Wilkie, T. M. (2000) *J. Biol. Chem.* **275,** 18962–18968
20. Tu, Y., and Wilkie, T. M. (2004) *Methods Enzymol.* **389,** 89–105
21. Davydov, I. V., and Varshavsky, A. (2000) *J. Biol. Chem.* **275,** 22931–22941
22. Hu, R. G., Sheng, J., Qi, X., Xu, Z., Takahashi, T. T., and Varshavsky, A. (2005) *Nature* **437,** 981–986
23. Lee, M. J., Tasaki, T., Moroi, K., An, J. Y., Kimura, S., Davydov, I. V., and Kwon, Y. T. (2005) *Proc. Natl. Acad. Sci. U. S. A.* **102,** 15030–15035
24. Drenan, R. M., Doupnik, C. A., Boyle, M. P., Muglia, L. J., Huettner, J. E., Linder, M. E., and Blumer, K. J. (2005) *J. Cell Biol.* **169,** 623–633
25. Takida, S., Fischer, C. C., and Wedegaertner, P. B. (2005) *Mol. Pharmacol.* **67,** 132–139
26. Hiol, A., Davey, P. C., Osterhout, J. L., Waheed, A. A., Fischer, E. R., Chen, C. K., Milligan, G., Druey, K. M., and Jones, T. L. (2003) *J. Biol. Chem.* **278,** 19301–19308
27. Osterhout, J. L., Waheed, A. A., Hiol, A., Ward, R. J., Davey, P. C., Nini, L., Wang, J., Milligan, G., Jones, T. L., and Druey, K. M. (2003) *J. Biol. Chem.* **278,** 19309–19316
28. Castro-Fernandez, C., Janovick, J. A., Brothers, S. P., Fisher, R. A., Ji, T. H., and Conn, P. M. (2002) *Endocrinology* **143,** 1310–1317
29. Rose, J. J., Taylor, J. B., Shi, J., Cockett, M. I., Jones, P. G., and Hepler, J. R. (2000) *J. Neurochem.* **75,** 2103–2112
30. Tu, Y., Popov, S., Slaughter, C., and Ross, E. M. (1999) *J. Biol. Chem.* **274,** 38260–38267
31. Druey, K. M., Ugur, O., Caron, J. M., Chen, C. K., Backlund, P. S., and Jones, T. L. (1999) *J. Biol. Chem.* **274,** 18836–18842
32. Tu, Y., Wang, J., and Ross, E. M. (1997) *Science* **278,** 1132–1135
33. De Vries, L., Elenko, E., Hubler, L., Jones, T. L., and Farquhar, M. G. (1996) *Proc. Natl. Acad. Sci. U. S. A.* **93,** 15203–15208
34. Tang, K. M., Wang, G. R., Lu, P., Karas, R. H., Aronovitz, M., Heximer, S. P., Kaltenbronn, K. M., Blumer, K. J., Siderovski, D. P., Zhu, Y., and Mendelsohn, M. E. (2003) *Nat. Med.* **9,** 1506–1512
35. Heximer, S. P., Watson, N., Linder, M. E., Blumer, K. J., and Hepler, J. R. (1997) *Proc. Natl. Acad. Sci. U. S. A.* **94,** 14389–14393
36. Heximer, S. P., Srinivasa, S. P., Bernstein, L. S., Bernard, J. L., Linder, M. E., Hepler, J. R., and Blumer, K. J. (1999) *J. Biol. Chem.* **274,** 34253–34259
37. Sinnarajah, S., Dessauer, C. W., Srikumar, D., Chen, J., Yuen, J., Yilma, S., Dennis, J. C., Morrison, E. E., Vodyanoy, V., and Kehrl, J. H. (2001) *Nature* **409,** 1051–1055
38. Roy, A. A., Lemberg, K. E., and Chidiac, P. (2003) *Mol. Pharmacol.* **64,** 587–593
39. Salim, S., Sinnarajah, S., Kehrl, J. H., and Dessauer, C. W. (2003) *J. Biol. Chem.* **278,** 15842–15849
40. Bernstein, L. S., Ramineni, S., Hague, C., Cladman, W., Chidiac, P., Levey, A. I., and Hepler, J. R. (2004) *J. Biol. Chem.* **279,** 21248–21256
41. Hague, C., Bernstein, L. S., Ramineni, S., Chen, Z., Minneman, K. P., and Hepler, J. R. (2005) *J. Biol. Chem.* **280,** 27289–27295
42. Roy, A. A., Baragli, A., Bernstein, L. S., Hepler, J. R., Hebert, T. E., and Chidiac, P. (2006) *Cell. Signal.* **18,** 336–348
43. Wang, X., Zeng, W., Soyombo, A. A., Tang, W., Ross, E. M., Barnes, A. P., Milgram, S. L., Penninger, J. M., Allen, P. B., Greengard, P., and Muallem, S. (2005) *Nat. Cell Biol.* **7,** 405–411
44. Grant, S. L., Lassegue, B., Griendling, K. K., Ushio-Fukai, M., Lyons, P. R., and Alexander, R. W. (2000) *Mol. Pharmacol.* **57,** 460–467
45. Kehrl, J. H., and Sinnarajah, S. (2002) *Int. J. Biochem. Cell Biol.* **34,** 432–438
46. Siderovski, D. P. (2004) *AfCS-Nature Molecule Pages* doi:10.1038/mp.a000028.01
47. Takata, S., Hirata, Y., Takagi, Y., Fukase, M., and Fujita, T. (1990) *Am. J. Hypertens.* **3,** 227S–230S
48. Kanaide, H., Ichiki, T., Nishimura, J., and Hirano, K. (2003) *Circ. Res.* **93,** 1015–1017
49. Jerius, H., Beall, A., Woodrum, D., Epstein, A., and Brophy, C. (1998) *Surgery* **123,** 46–50
50. Heximer, S. P., Knutsen, R. H., Sun, X., Kaltenbronn, K. M., Rhee, M. H., Peng, N., Oliveira-dos-Santos, A., Penninger, J. M., Muslin, A. J., Steinberg, T. H., Wyss, J. M., Mecham, R. P., and Blumer, K. J. (2003) *J. Clin. Invest.* **111,** 445–452
51. Sun, X., Kaltenbronn, K. M., Steinberg, T. H., and Blumer, K. J. (2005) *Mol. Pharmacol.* **67,** 631–639
52. Araki, T., Sasaki, Y., and Milbrandt, J. (2004) *Science* **305,** 1010–1013
53. Butt, E., Nolte, C., Schulz, S., Beltman, J., Beavo, J. A., Jastorff, B., and Walter, U. (1992) *Biochem. Pharmacol.* **43,** 2591–2600
54. Moneer, Z., Dyer, J. L., and Taylor, C. W. (2003) *Biochem. J.* **370,** 439–448
55. Moneer, Z., Pino, I., Taylor, E. J., Broad, L. M., Liu, Y., Tovey, S. C., Staali, L., and Taylor, C. W. (2005) *Biochem. J.* **389,** 821–829
56. Moneer, Z., and Taylor, C. W. (2002) *Biochem. J.* **362,** 13–21
57. Taylor, C. W. (2002) *Novartis. Found. Symp.* **246,** 91–107
58. Taylor, C. W., and Moneer, Z. (2004) *Biol. Res.* **37,** 641–645
59. Brueggemann, L. I., Markun, D. R., Barakat, J. A., Chen, H., and Byron, K. L. (2005) *Biochem. J.* **388,** 237–244
60. Brueggemann, L. I., Markun, D. R., Henderson, K. K., Cribbs, L. L., and Byron, K. L. (2006) *J. Pharmacol. Exp. Ther.* **317,** 488–499
61. He, T. C., Zhou, S., da Costa, L. T., Yu, J., Kinzler, K. W., and Vogelstein, B. (1998) *Proc. Natl. Acad. Sci. U. S. A.* **95,** 2509–2514
62. Luker, G. D., Sharma, V., Pica, C. M., Prior, J. L., Li, W., and Piwnica-Worms, D. (2003) *Cancer Res.* **63,** 1780–1788
63. Gill, D. L., and Patterson, R. L. (2004) *Sci. STKE 2004*, pe39

64. Oancea, E., Teruel, M. N., Quest, A. F., and Meyer, T. (1998) *J. Cell Biol.* **140,** 485–498
65. Butt, E., Eigenthaler, M., and Genieser, H. G. (1994) *Eur. J. Pharmacol.* **269,** 265–268
66. Hofmann, F., Feil, R., Kleppisch, T., and Schlossmann, J. (2006) *Physiol. Rev.* **86,** 1–23
67. Heximer, S. P., Lim, H., Bernard, J. L., and Blumer, K. J. (2001) *J. Biol. Chem.* **276,** 14195–14203
68. Gohla, A., Schultz, G., and Offermanns, S. (2000) *Circ. Res.* **87,** 221–227
69. Bodenstein, J., Sunahara, R. K., and Neubig, R. R. (2007) *Mol. Pharmacol.* **71,** 1040–1050
70. Schoeber, J. P., Topala, C. N., Wang, X., Diepens, R. J., Lambers, T. T., Hoenderop, J. G., and Bindels, R. J. (2006) *J. Biol. Chem.* **281,** 29669–29674
71. Wang, X., Zeng, W., Kim, M. S., Allen, P. B., Greengard, P., and Muallem, S. (2007) *EMBO J.* **26,** 2768–2776
72. Tikhonova, I. G., Boulegue, C., Langer, I., and Fourmy, D. (2006) *Biochem. Biophys. Res. Commun.* **341,** 715–720
73. Thuillez, C., and Richard, V. (2005) *J. Hum. Hypertens.* **19,** Suppl. 1, 21–25